THIS DOCUMENT PROVIDED BY THE ABBOTT AEROSPACE
TECHNICAL LIBRARY
ABBOTTAEROSPACE.COM

R. & M. No. 3362

LIBRARY
ROYAL AIRCRAFT ESTABLISHMENT
BEDFORD.

MINISTRY OF AVIATION

AERONAUTICAL RESEARCH COUNCIL
REPORTS AND MEMORANDA

Rolling-Power Tests on an Elastic Model Wing (M-Planform) in Low-Speed Flow

By D. R. Gaukroger, J. K. Curran and A. T. Marriot

LONDON: HER MAJESTY'S STATIONERY OFFICE
1964
FOURTEEN SHILLINGS NET

THIS DOCUMENT PROVIDED BY THE ABBOTT AEROSPACE
TECHNICAL LIBRARY
ABBOTTAEROSPACE.COM

Rolling-Power Tests on an Elastic Model Wing (M-Planform) in Low-Speed Flow

By D. R. Gaukroger, J. K. Curran and A. T. Marriot

Communicated by the Deputy Controller Aircraft (Research and Development), Ministry of Aviation

*Reports and Memoranda No. 3362**
August, 1962

Summary.

Measurements and calculations of aileron effectiveness for an elastic model wing in low-speed flow are described. The experimental technique enabled rolling moments due to applied aileron and to rate of roll to be measured separately. Rolling moments were also calculated using measured flexibility coefficients and factored two-dimensional steady-flow aerodynamic derivatives. Experimental and calculated results were in good agreement.

The wing tested was of M-planform, with two pairs of ailerons covering the inboard and outboard sections of the outer panels. The inboard ailerons were associated with a lower loss of control effectiveness.

LIST OF CONTENTS

* Replaces R.A.E. Report No. Structures 280—A.R.C. 24 442.

THIS DOCUMENT PROVIDED BY THE ABBOTT AEROSPACE
TECHNICAL LIBRARY
ABBOTTAEROSPACE.COM

LIST OF CONTENTS—*continued*

LIST OF APPENDICES

LIST OF TABLES

LIST OF ILLUSTRATIONS

THIS DOCUMENT PROVIDED BY THE ABBOTT AEROSPACE
TECHNICAL LIBRARY
ABBOTTAEROSPACE.COM

LIST OF ILLUSTRATIONS—*continued*

Figure

---

1. *Introduction.*

In the design of flap-type control surfaces for aircraft, consideration must be given to the aeroelastic problems that arise. Although, in practice, control-surface flutter is often the major problem, consideration must also be given to possible loss of control effectiveness. The theoretical side of the subject is well documented[1, 2, 3], but there appears to have been a notable lack of supporting experimental work in recent years. Current interest in wings of unconventional planform, and the need to assess aeroelastic problems associated with these designs, offered an opportunity to undertake an experimental programme on control effectiveness. The particular problem of interest was the performance of a wing of M-planform in respect of aileron effectiveness and rolling power.

A flexible model wing of M-planform was built, and its rolling characteristics were measured in a low-speed wind tunnel. The model was fitted with two pairs of ailerons of equal span which together extended over the whole of the outer panels of the wing; it was possible to apply either pair of ailerons separately, or both together. The characteristics measured were the values of rolling moment due to applied aileron, and rolling moment due to rate of roll. Estimates of these characteristics, based on measured stiffness coefficients for the wing, and using two-dimensional steady aerodynamic derivatives, were made. Comparison of experiment with calculation shows that good agreement is obtained for the general trends in behaviour; by applying a factor to the aileron aerodynamic derivatives good quantitative agreement between experiment and calculation may be obtained.

The programme included an investigation of divergence, and in this case good agreement was obtained between the experimental results and the calculations.

Two main conclusions emerge from the programme. The first, which relates to rolling tests generally, is that reliable results may be obtained from low-speed tests provided sufficient attention is paid to detail in the experiments. The second, relating particularly to the M-planform wing, is that unfavourable roll characteristics are likely to occur with an aileron that extends to the tip of the wing; on the other hand, an aileron just outboard of the wing kink is likely to be free of serious rolling-power losses.

THIS DOCUMENT PROVIDED BY THE ABBOTT AEROSPACE
TECHNICAL LIBRARY
ABBOTTAEROSPACE.COM

2. *Outline of Programme.*

2.1. The basic aim of the programme was to measure the rolling power of the model wing, and to compare this with the calculated performance. The straight-forward way of measuring rolling power is to measure the steady rate of roll achieved by the model under applied aileron. A second way is to measure separately the components of rolling moment due to applied aileron and to rate of roll, and to obtain the rolling power from the two values. In the present tests both methods were used, but for reasons explained in Section 5.1, attention was concentrated on the second method. In the case of a wing freely rolling under applied aileron (that is to say, with no externally applied rolling moment) the rolling moment due to applied aileron must equal the rolling moment due to rate of roll. Thus, from a knowledge of the rate of roll and of the rolling moment due to applied aileron, the rolling moment due to rate of roll can be obtained. It was considered, however, that a technique in which the rolling moment due to rate of roll is measured directly would be preferable to one that depends upon the measurement of rolling moment due to applied aileron. A technique was devised that satisfied this requirement, and the bulk of the information from the wind-tunnel tests consisted of values of the two aerodynamic rolling moments for each condition of windspeed and applied aileron.

2.2. The method of obtaining the rolling moment due to applied aileron was to measure the external rolling moment required to prevent roll.

The rolling moment due to rate of roll was obtained for each windspeed by applying a succession of external rolling moments to the model, and measuring in each case the resulting rate of roll. It is shown in Appendix II that the rolling moment due to rate of roll is proportional to the rate of change of applied rolling moment with rate of roll. It was found that this rate of change, and hence the value of the rolling moment due to rate of roll, is independent of the aileron angle.

In the calculation of rolling characteristics, it was obviously desirable that values of the two aerodynamic rolling moments should be obtained separately to enable a detailed comparison with the experiments to be made. The method of analysis is given in Appendix I.

2.3. The model was fitted with two pairs of ailerons of equal span, extending from the wing kink to the tip. Aileron settings relative to the wing at aileron mid-span of zero, 5° or 10° were represented for each section of the aileron, or for both sections simultaneously. Three aileron arrangements were investigated.

(i) Inboard ailerons only applied

(ii) Outboard ailerons only applied; and

(iii) Both pairs of ailerons applied.

In the latter case the inboard and outboard pairs of ailerons were applied through equal angles, and in no case were different settings of the two pairs investigated. Rolling moments due to applied aileron, and to rate of roll, were obtained at windspeeds from 40 to 140 ft/sec in increments of 20 ft/sec. In some cases the upper limit of this speed range was increased. In addition, the rate of roll in the freely rolling case was measured for each aileron arrangement. It was also necessary to repeat all the measurements with zero applied aileron to eliminate effects due to asymmetry. This was necessary at each value of windspeed, since the rolling moment due to asymmetry will not be proportional to the dynamic pressure, as the asymmetry itself introduces a mode of distortion of the model.

THIS DOCUMENT PROVIDED BY THE ABBOTT AEROSPACE
TECHNICAL LIBRARY
ABBOTTAEROSPACE.COM

3. *Details of Model and Test Rig.*

The model consisted of two half-wings (fuselage side to tip) which were bolted into a central cylindrical body representing the fuselage. The planform geometry is shown in Fig. 1. Each half-wing consisted of a single Duralumin spar which was tapered in both width and depth giving a stiffness distribution based on those of a design study for an aircraft of this planform. A note on the model scale is given in Appendix III. Each spar was made in two parts, which were locked into a connecting piece at the kink. The wing contour was provided by 12 segments, each of which was attached to the spar. Six of the segments made up the panel of the wing inboard of the kink, and six the outboard panel, all segments having an equal spanwise dimension. A thirteenth segment, representing a fuel tank or nacelle, was attached to the wing spar at the kink. All thirteen segments were constructed of wood, and for ease of assembly each segment could be subdivided into two sections forming the top and bottom surfaces of the wing. To give a rigid attachment between segment and spar, the latter was provided with branches extending in a fore-and-aft direction at each segment attachment point. Fig. 2 shows a half-wing during assembly; two of the inboard segments have been attached, and the next two have been partly attached, whilst the construction of the spar is shown over the adjacent segments. Each of the ailerons on the outboard panel was equal in spanwise dimension to three wing segments. In order to avoid any stiffness between the segments, other than that provided by the spar, each aileron was attached only to the centre segment of its span. Each aileron and its connecting plate was machined in aluminium from the solid, a separate aileron being required for each aileron angle. Fig. 2 shows an outboard aileron in position. Whilst every effort was made in design and manufacture to avoid large gaps between the segments, and between ailerons and segments, it was considered advisable to seal these gaps in order to avoid unrepresentative flow conditions. This was done by gluing thin rubber strips over the gaps in such a way that they would not contribute to stiffness over a reasonable range of inter-segment movement.

The root end of each spar terminated in an integral machined block, which was bolted into the central body or fuselage. The wind-tunnel rig consisted of a central rod supported by self-aligning bearings housed in fixed fairings at nose and tail. The portion of the fuselage free to roll formed a cylinder between the fairings, and was rigidly attached to the central rod (Fig. 3). The system was held in the wind tunnel by rigging wires attached to the nose and tail fairings. The fuselage itself had a plywood skin that could be removed for the adjustment of balance weights within. In rigging the model for test in the wind tunnel, care was taken in the alignment of the two bearings in order to obtain minimum friction in rotation.

External rolling moments were applied to the model by attaching a thin cord to the fuselage, and then taking it round the fuselage for a number of turns before leading it off to a pulley and scale pan outside the airstream. The arrangement is shown diagrammatically in Fig. 4.

The rate of roll of the model was measured by comparing a signal from a proximity-type transducer on the fuselage with a known time base. The transducer consisted of a fixed- and moving-plate condenser; the fixed plate was attached to the tail fairing, whilst the moving plate consisted of a serrated disc fixed to the rotating fuselage. The change of capacity as the serrations passed the fixed plate was converted to a voltage change, and displayed on an oscilloscope.

The divergence characteristics of the wing were investigated with the root rigidly held by measuring the change of frequency of the mode leading to divergence as the airspeed was increased. At wind speeds approaching the divergence speed, the mode that will eventually lead to divergence

THIS DOCUMENT PROVIDED BY THE ABBOTT AEROSPACE
TECHNICAL LIBRARY
ABBOTTAEROSPACE.COM

normally has the lowest frequency; hence it is only necessary to provide the wing with a simple disturbance, and to measure the lowest frequency of oscillation. A resulting graph of the square of the frequency plotted against the square of the windspeed may be extrapolated to obtain the divergence speed, which occurs when the natural frequency in the mode leading to divergence has fallen to zero. To measure the wing response in the divergence tests, strain gauges were attached to the spar near the root. The signals from these gauges were recorded against a known time base, and the records were analysed to obtain frequency of response to a wing disturbance.

4. *Still-Air Tests.*

4.1. *Rig Damping.*

The frictional rolling moment in the bearings was estimated in two ways. The wing was replaced by a wooden disc having the same rolling moment of inertia, and the first method consisted of applying external rolling moments and measuring the steady rate of roll achieved by the fuselage and the disc. The second method consisted of measuring the deceleration of fuselage and disc after an initial acceleration. The results from both these methods of test indicated that the frictional rolling moment in the bearings was practically constant within the range of rate of roll that the tests covered. Moreover this rolling moment, which was of the order of 0·0004 lb. ft, was small compared to the rolling moments measured in the wind-tunnel tests.

4.2. *Flexibility Coefficients.*

Flexibility coefficients for the model were measured on a half-wing, with spot checks on the other wing. These checks showed that both wings were of nearly identical stiffness, and justified the assumption of structural similarity made in the calculations.

In order to calculate the rolling characteristics of a flexible wing it is necessary to know, for each spanwise strip of the wing, the twist of the strip (in a plane parallel to the plane of symmetry) due to a moment (in the same plane) applied at that or any other strip, and also the twist due to a point load applied at that or any other strip. This information may be obtained as follows.

A moment in a plane parallel to the plane of symmetry is applied to one strip and the resultant twist of all strips is measured. Also, there will be a point Q_0 somewhere in the loaded section which is not displaced when the moment is applied, and the position of this point is measured. These measurements are repeated with the moment applied to another strip, and are continued until each strip has been separately loaded. The locus of the points Q_0 may be termed the 'Q_0 line' following the terminology used by Broadbent[3]. It may be noted that the application of a load at any point on the Q_0 line will produce no twist of the section at the loading point.

With a segmented model, the choice of spanwise strips is clearly determined by the segment geometry. With a wing of unusual planform, there is a clear case for making the measurements of flexibility as detailed as possible by loading and measuring at every segment. Unfortunately, in the tests described here, the time and effort required to do this were prohibitive. Seven segments were selected out of the thirteen available, three on the inboard panel of the wing, and three on the outboard, the seventh being the nacelle segment. The wing was rigidly held at the root end and at each of these segments four moments in planes parallel to the plane of symmetry were successively applied; for each moment the twist at every segment (including the loaded segment) was measured. The twists were computed from measurements of displacements of two points on the segment centre-line a known distance apart, the displacements being measured with capacity-type transducers.

THIS DOCUMENT PROVIDED BY THE ABBOTT AEROSPACE
TECHNICAL LIBRARY
ABBOTTAEROSPACE.COM

The measurements, after plotting and smoothing, gave a matrix of flexibilities for the seven segments in terms of twist at any segment due to unit moment at any segment. This was interpolated to obtain a similar matrix for all thirteen segments. First, the diagonal terms of the matrix (representing twist at each segment due to load at that segment) were plotted against a spanwise co-ordinate and the diagonal terms for the remaining six segments were interpolated. Second, since the matrix should be symmetrical and since the twist at each segment outboard of the loaded segment should be equal to the twist of the loaded segment, it would have been possible to have completed the thirteen segment matrix with the interpolated values for the main diagonal. However, in practice, the measured twists outboard of the loaded segment generally showed some variation from the twist at the loaded segment, and it was decided to complete the larger matrix by taking a mean of the measurements in the appropriate rows and columns. The matrix obtained is given in Table 1.

The Q_0 line was obtained from the experiments as the locus of points in each segment which were not displaced when a moment was applied to the segment. The position of the Q_0 line relative to the spar was obtained by interpolation for those segments on which no measurements were made. The locus of the line is shown in Fig. 5.

At this stage it is possible to calculate a matrix of twists due to point loads on the Q_0 line. For a point load on the line at a particular segment, there is no twist of that segment, and therefore in theory no twist of segments outboard of it. A segment inboard of it, however, experiences a load pattern equivalent to a load on the Q_0 line at the segment plus a moment, whose magnitude is proportional to the fore-and-aft distance between the positions of the Q_0 line at that segment and at the loaded segment. This moment produces a twist, the amplitude of which may be evaluated from the matrix of twists due to applied moments. It is possible in this way to calculate the matrix of twists due to point loads on the Q_0 line, and this has been done in the present case, giving the matrix of Table 2.

5. *Wind-Tunnel Tests.*

An outline of the programme of wind-tunnel tests has already been given in Section 2. Further details are given in this section, together with an indication of some of the practical problems encountered.

5.1. *Rolling Tests.*

In preparing the model for wind-tunnel tests, it was necessary to ensure that the centre of gravity of the rolling parts coincided with the axis of roll. It was, however, impossible to achieve this for all angular positions of the wings, since gravitational forces produced a droop of the wings in the horizontal position, and a 'yawing' distortion in the vertical position. In practice, the yawing distortion could be ignored in its effect on centre of gravity, but the drooping distortion produced significant effects.

An important effect of the wing droop was that at low rates of roll there could be a significant variation of rate of roll per cycle. Also, in rolling freely under applied aileron in conditions where the rate of roll was small, the rolling moment due to the gravitational effect with the wings horizontal could be large enough to overcome the net aerodynamic rolling moment, and so prevent roll altogether. This effect was minimised in two ways. In measuring the rolling moment due to applied aileron (i.e. the external moment necessary to prevent roll) the measurements were made with the wings vertical. In measuring the rolling moment due to rate of roll (by applying external moments

THIS DOCUMENT PROVIDED BY THE ABBOTT AEROSPACE
TECHNICAL LIBRARY
ABBOTTAEROSPACE.COM

and measuring rate of roll) sufficiently large moments were applied to ensure a reasonably constant rate of roll per cycle. In practice this usually required that the rate of roll should not fall below about 1·5 radians per second.

It is interesting to note one or two further effects of gravitational droop. With the wings horizontal in the windstream the droop mode is modified by the aerodynamic forces, and may result in increased droop and a further lowering of the wing centre of gravity, which in turn leads to a larger 'gravitational' rolling moment. Some measure of this effect may be seen in Fig. 6, in which the external rolling moment required to prevent roll with applied aileron is shown plotted against windspeed for four angular positions of the wing, two vertical and two horizontal. It will be noted that the differences between the curves vary with windspeed. In analysing the test results the mean of the values with the wings vertical was taken as the best value of rolling moment due to applied aileron. If the model is allowed to roll freely under applied aileron the effective values of the rolling-moment terms in the equation of motion are continuously varying throughout each cycle and are only equal to their true values when the wings are vertical. The mean rate of roll is, in fact, always an underestimate of the rate of roll the model would achieve under ideal conditions. This gives an additional, and very strong, reason for computing the 'ideal' rate of roll from the separate measurements of rolling moments due to rate of roll and to applied aileron, since the gravitational effects can be largely eliminated in the separate measurements.

5.2. *Divergence.*

The divergence measurements have been mentioned in Section 3. Interest in the divergence characteristics of the wing arose from a divergence that occurred during initial testing of the model. At the time, the model was being tested in free roll under applied aileron, and the wind-tunnel speed was being incrementally increased. Without warning, at approximately 200 feet per second, both wings diverged symmetrically, and only prompt action by the tunnel operator prevented irreparable damage to the model. The divergence was interesting in that both wings behaved almost identically, diverging at the same instant and through the same amplitude. Fig. 7 is a photograph of the model after divergence; the similarity in wing modes is clearly shown. Fig. 8 shows the spar distortion and indicates that the main distortion was bending of the inner wing near to the root. The spar was straightened under heat treatment and was used for all the subsequent tests. After repair, the flexibility coefficients were measured (Section 4.3) and were followed by the wind-tunnel divergence tests in order to establish a safe maximum operating speed. The frequency of the mode of lowest damping was measured, as described in Section 3, and Fig. 9 shows a plot of the square of the mode frequency against the square of the windspeed. If the structural stiffness in the mode leading to divergence is e, the inertia a and the aerodynamic stiffness c, then the frequency of the mode at a windspeed V is given by:

$$\omega^2 = \frac{e + cV^2}{a}.$$

Thus, if the mode shape does not change appreciably a graph of V^2 against ω^2 will be a straight line cutting the V^2 axis (when $\omega^2 = 0$) at the divergence speed. It is, of course, a requirement for divergence to occur that the sign of c should be negative. The second curve in Fig. 9 was obtained with added mass in the nacelle. The reason for this was that some difficulty was experienced at the higher speeds in obtaining a reliable frequency from a rapidly damped response to disturbance; by adding inertia, the response was extended sufficiently to enable frequencies to be measured at a

THIS DOCUMENT PROVIDED BY THE ABBOTT AEROSPACE
TECHNICAL LIBRARY
ABBOTTAEROSPACE.COM

rather higher windspeed (an increase of 20 feet per second). Extrapolation of the measured values gives divergence speeds of 263 and 238 feet per second, the latter being the more reliable estimate.

6. *Calculations.*

6.1. The analysis used in the calculations is given in Appendix I, and it will be seen that the results obtained give the variation of three non-dimensional parameters with windspeed. The first of these parameters, denoted by X, is defined as the ratio of the rate of roll achieved by the model in the freely rolling condition under applied aileron to the rate of roll of a rigid but otherwise identical model under the same conditions. X is sometimes referred to as the 'rolling effectiveness' and is the parameter whose variation is normally investigated in rolling-power calculations[1, 2, 3]. The second parameter Y is defined as the ratio of the aileron angle that must be applied on the model to prevent roll under an applied external rolling moment to the aileron angle that must be applied on a rigid but otherwise identical model subject to the same external rolling moment. The third parameter, Z, is defined as the ratio of the rate of roll achieved by the model with zero applied aileron but subject to an applied external rolling moment, to the rate of roll achieved by a rigid but otherwise identical model subject to the same external rolling moment. It is shown in Appendix I that:

$$X = \frac{Z}{Y}.$$

The programme of calculations consisted of solving equations (20), (24) and (29) of Appendix I to obtain the variation of X, Y and Z with airspeed, and also the twist modes in each case. The calculations were made on a 'Mercury' computer and provision was made in the programme for obtaining the first positive latent root of each equation. This was necessary because in some cases the first latent root was negative (corresponding to a negative value of dynamic pressure). This occurred in solving the equations for Z variation, and in solving for X and Y for the inboard aileron only.

Solutions were obtained (i) with inboard ailerons only, (ii) with outboard ailerons only, and (iii) with both pairs of ailerons. Strictly, it is unnecessary to compute all three cases, since the third can be obtained from any two. Nor is it necessary to compute for X, Y and Z; again, any two are sufficient, but having prepared a general programme for the computer, little extra work was needed to obtain all the solutions, and it was then possible to make a check on the results.

6.2. The data on which the calculations were based consisted of the wing geometry, the measured values of flexibility coefficients and aerodynamic terms. To obtain the latter values, a rigid model was built and tested. The intention was to obtain values of rolling moment due to applied aileron, and to rate of roll, from the tests on the rigid model and to use these, in conjunction with theoretical distribution of lift and moment, in the calculations on the flexible model. The rigid model was built of solid mahogany, and spot checks of stiffness showed that the ratio of the stiffness to that of the flexible model was of the order of fifty to one.

The rolling moment due to rate of roll for the rigid model was measured by the method of Section 2.2. A spanwise distribution of a_1, calculated for the planform for a uniform-pitch mode, was assumed[4], and a value of a_1 for the nacelle was calculated using slender-body theory. The value of the coefficient for rolling moment due to rate of roll was evaluated from this data and was compared with the measured value for the rigid model. A factor was then applied to the theoretical values in order to equate the two. The factored values of a_1 derived in this way are shown in Fig. 10a.

THIS DOCUMENT PROVIDED BY THE ABBOTT AEROSPACE
TECHNICAL LIBRARY
ABBOTTAEROSPACE.COM

Owing to manufacturing differences between the ailerons of the flexible and rigid wings, it was decided not to use the rigid-wing measurements of rolling moment due to applied aileron as a basis for determining the aileron derivatives used in the calculations. Instead, these derivatives were determined on a semi-empirical basis. A distribution of aileron lift and moment based on two-dimensional theory was assumed, and it was also assumed that the centre of pressure under applied aileron (given by m/a_2) was the same as for the two-dimensional case. With these assumptions the rigid-wing rolling power $ps/V\beta$ was calculated in terms of a mean value of a_2. This power was equated to the power obtained from the tests on the flexible wing, so giving the mean value of a_2. The rigid-wing rolling power was obtained from the tests by extrapolating the curves of $ps/V\beta$ to zero windspeed, in which condition there is no effect of flexibility. The main drawback of this method is the difficulty of extrapolating the experimental results of Figs. 19 to 21 with any accuracy on account of the scatter. In practice, therefore, the calculations giving the variation of rolling effectiveness X with airspeed were made using an arbitrary mean value of a_2; the variation of $ps/V\beta$ was then calculated and a factor (constant with windspeed) was found which could be applied to the calculated values to give the best agreement with the experiments. The mean value of a_2 required in the calculations to give this result directly (without the need to apply a factor) is simply the product of the assumed arbitrary value of a_2 and the factor itself. The justification for this procedure requires that the variation of X is independent of a_2. It is shown in Appendix I that this is so, provided a_2 is proportional to m and the distribution of a_2 remains constant—assumptions which, as mentioned above, were made in the calculations. In the present case there was little difficulty in fitting the calculated curve to the experimental results because of the agreement between the two sets of results in respect of wing flexibility effects. Had there not been agreement, however, the calculated curve would have differed in shape from the experimental results and matching would have been difficult if not impossible.

The values of a_2 determined by this method were $0{\cdot}50$ and $0{\cdot}27$ of the two-dimensional values for the inboard and outboard ailerons respectively and these were used in all the subsequent calculations. For the case with both pairs of ailerons applied, good agreement with experiment was obtained. The aileron lift distribution is shown in Fig. 10b with the two-dimensional values for comparison. Obviously a further refinement in the calculations would be to smooth the lift distribution of Fig. 10b so that a sharp step between inboard and outboard ailerons is avoided when both pairs of ailerons are applied simultaneously. In view of the scatter of the experimental results with which such calculations would have to be compared, however, this was not attempted.

7. *Comparison of Theory and Experiment.*

7.1. *Rolling Moment due to Applied Aileron.*

The variation of rolling moment per unit aileron angle with airspeed for the inboard pair of ailerons is shown in Fig. 11.

The two sets of points give the measured values, and the full line the calculated values using the method of Appendix II. The figure shows quite good agreement. The fact that the 5° aileron values are, in all but one case, greater than the 10° may indicate a manufacturing error in the ailerons or in their attachment system.

The corresponding curve for the outboard ailerons is shown in Fig. 12. Here there is greater scatter of the experimental results, although the agreement with calculation, particularly near reversal, is not unreasonable.

THIS DOCUMENT PROVIDED BY THE ABBOTT AEROSPACE
TECHNICAL LIBRARY
ABBOTTAEROSPACE.COM

The results for both pairs of ailerons are shown in Fig. 13. The calculated curve is, of course, the sum of the curves of Figs. 11 and 12, and agreement with experiment is reasonable except at the maximum speed tested.

The calculated variation of the parameter Y with airspeed (V) from which the calculated moments were derived, is shown in Fig. 14 for all three aileron cases. It will be noted that Y is unity at $V = 0$, and rises as V increases; it becomes infinite at the reversal speed and then changes sign, becoming zero at the divergence speed. The modes of wing twist in the plane of symmetry at 100 feet per second are shown in Fig. 15 for unit twist at the wing kink. It will be seen that the application of inboard aileron produces positive twist over part of the wing and negative over the remainder, whereas the mode for the outboard aileron has the same sign over the whole wing. One would expect, therefore, that the wing mode due to application of inboard ailerons would be to some extent self-cancelling in respect of rolling moment produced, whereas that due to the outboard aileron would not. In other words, on the basis of mode shape it might be expected that the effectiveness of the inboard aileron would be less influenced by aeroelasticity than the outboard aileron.

7.2. *Rolling Moment due to Rate of Roll and Divergence.*

The slope of the line obtained by plotting external rolling moment against rate of roll was measured for the six cases with applied aileron, and the case with zero aileron. The values of rolling moment per unit rate of roll are plotted against airspeed in Fig. 16, which includes all the experimental results. The full line denotes the calculated values, and it will be seen that the line represents a fair mean of the experimental values except at the lower speeds.

The variation of the parameter Z with airspeed V is shown in Fig. 17. At $V = 0$, Z is unity, and does not change much in value up to 100 feet per second; thereafter it falls steadily to zero at the divergence speed. The shape of the wing twist modes at 100, 150, 200 feet per second and at divergence are shown in Fig. 18. It may be noted that at divergence the model cannot in theory be made to roll, because the twist amplitude will increase to counteract any applied rolling moment.

It can be deduced that the complete model must diverge symmetrically in the freely rolling condition. For antisymmetric conditions at speeds above that for symmetric divergence the model would simply achieve a rate of roll such that a balance between aerodynamic and elastic forces was achieved. But this would not be a divergent condition. Since the aerodynamic loading due to a symmetrical divergence cannot be relieved by rolling, and the model cannot translate, symmetrical divergence will occur at the fixed-root divergence speed.

The divergence tests are described in Section 5.2 and the extrapolated value of 238 feet per second (Fig. 9) compares very well indeed with the calculated value of 235 feet per second. It is not known why the model originally diverged at about 200 feet per second, but it has been suggested that the rubber strips between segments may have been attached in such a way that they adversely affected the stiffness distribution. Certainly, less care to avoid stiffness effects was exercised in the initial fitting of these strips than was the case later.

7.3. *Free-Roll Characteristics.*

The variation of rolling power with airspeed for the three aileron arrangements is shown in Figs. 19, 20 and 21. The experimental points have been derived from the separate measurements of rolling moment as shown in Appendix II. The full lines show the calculated values. Since reasonable

THIS DOCUMENT PROVIDED BY THE ABBOTT AEROSPACE
TECHNICAL LIBRARY
ABBOTTAEROSPACE.COM

agreement was obtained between experiment and calculation for the separate aerodynamic rolling moments it is to be expected that rolling powers derived from these results will also be in agreement. A certain amount of scatter arises from the addition of errors in the two components. The calculated modes in free roll at 100 feet per second are shown in Fig. 22.

It may be noted that the analysis of Appendix I assumes that the aileron angle relative to the wing is constant along the aileron span. In the present tests the ailerons were attached to the wing at their mid-span sections only, so that the assumption of constant aileron angle is incorrect. Calculation of the wing distortions for a typical case, however, shows that the change of angle along the aileron span is very small. For applied inboard aileron at 200 feet per second with the wing freely rolling, the difference in angle at each end of the aileron amounts to no more than 0·5 degrees per radian of applied aileron.

The rolling-power curves throw some interesting light on the relative merits of inboard and outboard positions for an aileron on the outer panel of an M-wing. The effectiveness of the outboard aileron falls off rapidly with increase of speed whereas that of the inboard aileron is barely affected. Consequently the rolling power of the combined aileron is less than that of the inboard aileron alone above a certain speed.

8. *Conclusions.*

The programme of experiment and calculation has indicated some of the practical difficulties to be faced in making a quantitative investigation of the rolling characteristics of an elastic wing. On the experimental side, the whole technique of testing would have been improved had it been possible to make the tests in a vertical wind tunnel, so avoiding cyclical gravitational effects. On the other hand, the technique of external loading worked well in enabling values of rolling moment due to rate of roll to be measured independently of those due to applied aileron. The opportunity to obtain a theoretical check on each term of the rolling-moment equation is obviously advantageous and the slightly increased complexity of the analysis is not a disadvantage if digital-computing machinery is available. The agreement between theory and experiment is, in general, good, though this was only achieved by factoring the basic aerodynamics of the ailerons in the calculations so as to obtain agreement for the undistorted wing. Once this had been done, however, the effects of model flexibility were accurately predicted in the calculations.

In relation to the M-planform, it appears that an inboard aileron on the outer wing panel is much less affected by aeroelasticity than the outboard, and in a practical design would be preferred.

The agreement between the calculated divergence speed and that obtained by extrapolating experimental results is good, and, as a point of technique, the advantages to be gained from increasing the inertia of the wing in the divergence measurements are worth noting.

Acknowledgment.

The authors wish to acknowledge the valuable work done by Mr. A. J. Fielding of R.A.E. in laboratory and wind-tunnel tests.

THIS DOCUMENT PROVIDED BY THE ABBOTT AEROSPACE
TECHNICAL LIBRARY
ABBOTTAEROSPACE.COM

REFERENCES

No.	*Author(s)*	*Title, etc.*
1	A. R. Collar and E. G. Broadbent ..	The rolling power of an elastic wing. Parts I and II. A.R.C. R. & M. 2186. October, 1945.
2	E. G. Broadbent and Ola Mansfield	Aileron reversal and wing divergence of swept wings. A.R.C. R. & M. 2817. September, 1947.
3	E. G. Broadbent	The rolling power of an elastic swept wing. A.R.C. R. & M. 2857. July, 1950.
4	H. C. Garner and W. E. A. Acum ..	Theoretical subsonic derivatives for an oscillating M-wing. A.R.C. R. & M. 3214. January, 1959.

THIS DOCUMENT PROVIDED BY THE ABBOTT AEROSPACE
TECHNICAL LIBRARY
ABBOTTAEROSPACE.COM

APPENDIX I

Analytical Treatment

AI.1. Let the wing be divided into a number of fore-and-aft strips, and using matrix notation let $\{L\}$ be the column matrix of lift forces and $\{M\}$ the column matrix of nose-up pitching moments in the streamwise direction about the Q_0 line (*see* Section 4.3).

AI.2. For the case in which the aileron angle is zero, a steady rate of roll is produced by an external rolling moment; the equation of rolling moments is:

$$\{y\}'\{L\} + R_z = 0 \tag{1}$$

where $\{y\}'$ is the row matrix of the spanwise dimensions y of the mid-point of a strip from the axis of roll, and R_z is the external rolling moment.

Now

$$\{L\} = \{L_z\}\theta_z - \{L_\eta\}\frac{ps}{V} \tag{2}$$

where

$\{L_z\}$ is the column of lift components due to distortion

θ_z is the twist of a reference section

$\{L_\eta\}$ is the column of lift components of the linear incidence mode due to rate of roll

p is the steady rate of roll

s is the distance from the roll axis to the wing tip

V is the airspeed.

The pitching-moment equation corresponding to (2) is:

$$\{M\} = \{M_z\}\theta_z - \{M_\eta\}\frac{ps}{V}. \tag{3}$$

Substituting for $\{L\}$ from equation (2) in equation (1):

$$\{y\}'\left(\{L_z\}\theta_z - \{L_\eta\}\frac{ps}{V}\right) + R_z = 0. \tag{4}$$

The corresponding equation for a rigid but otherwise identical wing subject to the same external rolling moment is:

$$-\{y\}'\{L_\eta\}\frac{p_R s}{V} + R_z = 0, \tag{5}$$

where p_R is the steady rate of roll for the rigid wing.

Let $Z = p/p_R$, then from equation (5):

$$R_z = \{y\}'\{L_\eta\}\frac{ps}{ZV}. \tag{6}$$

THIS DOCUMENT PROVIDED BY THE ABBOTT AEROSPACE
TECHNICAL LIBRARY
ABBOTTAEROSPACE.COM

Now from equation (4):

$$\theta_z = \frac{\{y\}'\{L_\eta\}\frac{ps}{V} - R_z}{\{y\}'\{L_z\}} \tag{7}$$

and substituting for R_z from equation (6) in equation (7):

$$\theta_z = \frac{\{y\}'\{L_\eta\}}{\{y\}'\{L_z\}}\left(1 - \frac{1}{Z}\right)\frac{ps}{V}. \tag{8}$$

AI.3. For the case in which positive aileron is applied, but roll prevented by an external rolling moment

$$\{L\} = \{L_y\}\theta_y + \{L_\beta\}\beta \tag{9}$$

where

$\{L_y\}$ is the column of lift components due to distortion

θ_y is the twist of a reference section

$\{L_\beta\}$ is the column of lift components due to applied aileron

β is the aileron angle which is assumed constant over the aileron span.

The moment equation corresponding to (9) is:

$$\{M\} = \{M_y\}\theta_y + \{M_\beta\}\beta. \tag{10}$$

The equation of rolling moments is:

$$\{y\}'\{L\} + R_y = 0 \tag{11}$$

where R_y is the external rolling moment.
Substituting for $\{L\}$ from equation (9) in equation (11):

$$\{y\}'(\{L_y\}\theta_y + \{L_\beta\}\beta) + R_y = 0. \tag{12}$$

The corresponding equation for a rigid but otherwise identical model subject to the same external rolling moment is:

$$\{y\}'\{L_\beta\}\beta_R + R_y = 0 \tag{13}$$

where β_R is the aileron angle of the rigid model.
Let $Y = \beta/\beta_R$, then from equation (13):

$$R_y = -\{y\}'\{L_\beta\}\frac{\beta}{Y}. \tag{14}$$

Now from equation (12):

$$\theta_y = -\frac{R_y + \{y\}'\{L_\beta\}\beta}{\{y\}'\{L_y\}} \tag{15}$$

and substituting for R_y from equation (14) in equation (15):

$$\theta_y = \frac{\{y\}'\{L_\beta\}}{\{y\}'\{L_y\}}\left(\frac{1}{Y} - 1\right)\beta. \tag{16}$$

THIS DOCUMENT PROVIDED BY THE ABBOTT AEROSPACE
TECHNICAL LIBRARY
ABBOTTAEROSPACE.COM

AI.4. The components of the aerodynamic forces L and M may be written non-dimensionally as follows:

$$\left.\begin{aligned}
\{L_\beta\} &= qc_r s\{l_\beta\} \quad \text{where} \quad \{l_\beta\} = \{a_2 c/c_r d\eta\} \\
\{L_y\} &= qc_r s\{l_y\} \quad \text{where} \quad \{l_y\} = \{a_1 c/c_r f_y d\eta\} \\
\{L_\eta\} &= qc_r s\{l_\eta\} \quad \text{where} \quad \{l_\eta\} = \{a_1 c/c_r \eta d\eta\} \\
\{L_z\} &= qc_r s\{l_z\} \quad \text{where} \quad \{l_z\} = \{a_1 c/c_r f_z d\eta\} \\
\{M_\beta\} &= qc_r^2 s\{m_\beta\} \text{ where } \{m_\beta\} = \{(ea_2 - m)(c/c_r)^2 d\eta\} \\
\{M_y\} &= qc_r^2 s\{m_y\} \text{ where } \{m_y\} = \{ea_1(c/c_r)^2 f_y d\eta\} \\
\{M_\eta\} &= qc_r^2 s\{m_\eta\} \text{ where } \{m_\eta\} = \{ea_1(c/c_r)^2 \eta d\eta\} \\
\{M_z\} &= qc_r^2 s\{m_z\} \text{ where } \{m_z\} = \{ea_1(c/c_r)^2 f_z d\eta\}
\end{aligned}\right\} \qquad (17)$$

and

q is the dynamic pressure ($= \frac{1}{2}\rho V^2$)

c_r is the reference chord of the wing

c is the local chord

ec is the distance of the Q_0 line aft of the aerodynamic centre

ηs is the distance from roll axis to a chordwise section

a_1 is $\dfrac{\partial C_L}{\partial \alpha}$

a_2 is $\dfrac{\partial C_L}{\partial \beta}$

m is $-\left(\dfrac{\partial C_M}{\partial \beta}\right)_{C_L \text{ constant}}$

f_y is the wing distortion mode in twist due to applied aileron

f_z is the wing distortion mode in twist due to rate of roll.

AI.5. The equation relating the local twist of the wing sections to the aerodynamic forces is

$$\{\theta\} = -[\theta]\{L\} + [\bar{\theta}]\{M\} \qquad (18)$$

where

$\{\theta\}$ is a column of twists

$[\theta]$ is the square flexibility matrix of nose-up twist due to unit download

$[\bar{\theta}]$ is the square flexibility matrix of nose-up twist due to unit nose-up moment.

For the case in which the aileron angle is zero and the wing rolls due to an external moment (Section AI.2), substitution for L and M from equations (2), (3) and (17) in equation (18) gives:

$$\{f_z\}\theta_z = qc_r s\left(-[\theta]\left(\{l_z\}\theta_z - \{l_y\}\frac{ps}{V}\right) + c_r[\bar{\theta}]\left(\{m_z\}\theta_z - \{m_y\}\frac{ps}{V}\right)\right) \qquad (19)$$

where $\{f_z\}\theta_z = \{\theta\}$.

THIS DOCUMENT PROVIDED BY THE ABBOTT AEROSPACE
TECHNICAL LIBRARY
ABBOTTAEROSPACE.COM

By substituting for $\{l_z\}$, $\{l_\eta\}$, $\{m_z\}$ and $\{m_\eta\}$ from equation (17) and for θ_z from equation (8), equation (19) may be reduced to:

$$\{f_z\} = qc_r s \left([\phi_1] + \frac{Z}{1-Z} [\phi_2] \right) \{f_z\} \tag{20}$$

where

$$[\phi_1] = - [\theta] [a_1 c/c_r d\eta] + c_r [\bar{\theta}] [e a_1 (c/c_r)^2 d\eta] \tag{21}$$

$$[\phi_2] = \frac{1}{\{\eta\}' \{a_1 c/c_r \eta d\eta\}} \left(\left(- [\theta] \{a_1 c/c_r \eta \, d\eta\} + \right. \right.$$
$$\left. \left. + c_r [\bar{\theta}] \{e a_1 (c/c_r)^2 \eta \, d\eta\} \right) \{a_1 c/c_r \eta \, d\eta\}' \right) \tag{22}$$

and $\{\}'$ denotes a row matrix, and $[a_1 \, c/c_r \, d\eta]$ and $[e a_1 \, (c/c_r)^2 \, d\eta]$ are diagonal matrices.

For the case in which positive aileron is applied, but roll prevented by an external rolling moment (Section AI.3) substitution for L and M from equations (9), (10) and (17) in equation (18) gives:

$$\{f_y\}\theta_y = qc_r s \left(- [\theta] \left(\{l_y\}\theta_y + \{l_\beta\}\beta \right) + c_r [\bar{\theta}] \left(\{m_y\}\theta_y + \{m_\beta\}\beta \right) \right) \tag{23}$$

where $\{f_y\}\theta_y = \{\theta\}$.

Again by substitution, equation (23) leads to:

$$\{f_y\} = qc_r s \left([\phi_1] + \frac{Y}{Y-1} [\phi_3] \right) \{f_y\} \tag{24}$$

where ϕ_1 is defined in equation (21)
and

$$[\phi_3] = \frac{1}{\{\eta\}' \{a_2 c/c_r d\eta\}} \left(\left([\theta] \{a_2 c/c_r d\eta\} - \right. \right.$$
$$\left. \left. - c_r [\bar{\theta}] \{(e a_2 - m)(c/c_r)^2 d\eta\} \right) [a_1 c/c_r \eta \, d\eta] \right). \tag{25}$$

Equations (20) and (24) may be solved by an iteration process to obtain the variation of Y and Z with q, and also the mode shapes $\{f_y\}$ and $\{f_z\}$.

AI.6. The freely rolling case can be considered as a combination of the cases dealt with in Sections AI.2 and AI.3 provided the external rolling moments in those cases are of equal magnitude and opposite sign, that is to say:

$$R_y = - R_z .$$

With this condition, adding equations (6) and (14) gives:

$$\{y\}' \{L_\beta\} \beta \frac{1}{Y} - \{y\}' \{L_\eta\} \frac{ps}{V} \frac{1}{Z} = 0 . \tag{26}$$

This equation relates the rate of roll p to the applied aileron angle β. The corresponding equation for a rigid but otherwise identical wing having the same applied aileron angle β is:

$$\{y\}' \{L_\beta\} \beta - \{y\}' \{L_\eta\} \frac{p_R s}{V} = 0 \tag{27}$$

THIS DOCUMENT PROVIDED BY THE ABBOTT AEROSPACE
TECHNICAL LIBRARY
ABBOTTAEROSPACE.COM

where p_R is the rate of roll of the rigid wing. In the conventional analysis the rolling effectiveness of the elastic wing is denoted by X, where $X = p/p_R$, and substituting for p_R in equation (27) gives:

$$\{y\}'\{L_\beta\}\beta - \{y\}'\{L_\eta\}\frac{ps}{V}\frac{1}{X} = 0. \tag{28}$$

This equation relates the rate of roll to the applied aileron angle in terms of the parameter X, whereas equation (26) gives the same relationship in terms of Y and Z. For equations (26) and (28) to have the same solution, $X = Z/Y$. The iterative equation arising from the conventional solution (using X) may be reduced to a form similar to that of equations (20) and (24). In this form it is:

$$\{f_x\} = qc_rs\left([\phi_1] + \frac{X}{1-X}[\phi_2] + \frac{1}{1-X}[\phi_3]\right)\{f_x\} \tag{29}$$

where $[\phi_1]$, $[\phi_2]$ and $[\phi_3]$ are as before, and $\{f_x\}$ is the mode shape in free roll.

The rolling power $ps/V\beta$ may be obtained from either equations (26) or (28):

$$\frac{ps}{V\beta} = \frac{\{\eta\}'\{l_\beta\}}{\{\eta\}'\{l_\eta\}}\frac{Z}{Y} = \frac{\{\eta\}'\{l_\beta\}}{\{\eta\}'\{l_\eta\}}X. \tag{30}$$

It may be noted that each of the $[\phi]$ matrices has a physical significance. The term in $[\phi_1]$ relates to the elastic response of the wing in an airstream when it is not rolling and no aileron is applied; the lowest positive latent root of the equation

$$\{f\} = qc_rs[\phi_1]\{f\} \tag{31}$$

gives the divergence speed of the wing. The term in $[\phi_2]$ relates to the response due to rate of roll, and the term in $[\phi_3]$ relates to the response due to applied aileron. $[\phi_3]$ is the only one of the three matrices containing the aileron derivatives a_2 and m, and it is interesting that if a_2 is proportional to m the solutions involving Y and X are independent of the aileron derivatives. The reason for this is that Y and X are ratios of performance relative to a similar but rigid wing, and varying the aileron derivatives affects both rigid and flexible wings to the same extent. But all the $[\phi]$ matrices are linearly dependent on a_1, and the effect of, say, doubling a_1 in the calculation would be to halve the value of q for the appropriate values of X, Y or Z.

The physical reason why equation (31) gives the divergence solution may be seen by considering equation (20). If Z is zero {giving equation (31)} this means that the rate of roll is zero even if an infinitely large external rolling moment is applied. This can only occur when the aerodynamic rolling moment, and hence the wing twist, are infinite, i.e. at divergence. Similarly if, in equation (24), Y is zero {giving equation (31) again} then the aileron angle required to prevent roll against an external rolling moment is zero, even if the external moment is infinitely large; this can only occur if the aerodynamic rolling moment is provided by infinite wing twist.

THIS DOCUMENT PROVIDED BY THE ABBOTT AEROSPACE
TECHNICAL LIBRARY
ABBOTTAEROSPACE.COM

APPENDIX II

Method of Comparison of Calculated and Experimental Results

AII.1. *Rolling Moment due to Applied Aileron.*

If the model is prevented from rolling under applied aileron by an external moment, then from equation (14) of Appendix I:

$$\frac{R_y}{\beta} = -\{y\}'\{L_\beta\}\frac{1}{Y} = -qc_r s^2\{\eta\}'\{l_\beta\}\frac{1}{Y}. \tag{32}$$

Values of R_y/β were obtained from the wind-tunnel tests and were compared with calculated values, obtained from the right-hand side of the equation.

AII.2. *Rolling Moment due to Rate of Roll.*

If the model is acted upon by an external rolling moment R this may be added to equation (26) of Appendix I to give:

$$\{y'\}\{L_\beta\}\beta\frac{1}{Y} - \{y\}'\{L_\eta\}\frac{ps}{V}\frac{1}{Z} + R = 0 \tag{33}$$

from which

$$\frac{dR}{dp} = \{y\}'\{L_\eta\}\frac{s}{VZ} = qc_r s^3\{\eta\}'\{l_\eta\}\frac{1}{VZ}. \tag{34}$$

Values of dR/dp were obtained from the wind-tunnel tests and were compared with calculated values obtained from the right-hand side of the equation.

AII.3. *Rolling Power.*

Rolling power was calculated from equation (30) of Appendix I and was compared with that obtained experimentally using the relationship:

$$\frac{ps}{V\beta} = -\frac{R_y/\beta}{dR/dp}\frac{s}{V}. \tag{35}$$

THIS DOCUMENT PROVIDED BY THE ABBOTT AEROSPACE
TECHNICAL LIBRARY
ABBOTTAEROSPACE.COM

APPENDIX III

Model Scale

AIII.1. For aeroelastic similarity between an aircraft and a model, a number of parameters must be satisfied. In the case of static aeroelastic phenomena, it is unnecessary to satisfy the mass parameter, and the stiffness ratio between the model and aircraft is determined by:

$$\left(\frac{E}{\rho V^2}\right)_{\mathrm{A}} = \left(\frac{E}{\rho V^2}\right)_{\mathrm{M}} \tag{36}$$

where

E is the modulus of elasticity

ρ is air density

V is airspeed,

and the suffixes A and M refer to the aircraft and model respectively.

In addition to equation (36) it is also necessary, of course, that the model shall be geometrically similar externally to the aircraft, and the stiffness distribution shall also be the same for model and aircraft.

Denoting the ratio aircraft length divided by model length by λ, equation (36) becomes:

$$\frac{V^2_{\mathrm{M}}}{V^2_{\mathrm{A}}} = \frac{(EI)_{\mathrm{M}}}{(EI)_{\mathrm{A}}} \frac{\rho_{\mathrm{A}}}{\rho_{\mathrm{M}}} \lambda^4. \tag{37}$$

Equation (37) gives the speed scale as a function of the rigidity EI, air density ρ and linear scale λ.

AIII.2. The model tested was designed to represent an aircraft which had been the subject of a design study. The aircraft span was 134 feet, and maximum E.A.S. was 450 knots. Owing to the need to design a model spar whose manufacture was reasonably simple, the stiffness distributions of model and aircraft were not identical. To show the order of the speed scale of the experiment however, it is assumed that:

$$\frac{(EI)_{\mathrm{A}}}{(EI)_{\mathrm{M}}} \simeq 10^8.$$

This value is reasonable over the greater part of the wing span, but is somewhat high at the wing tip.

Substituting the above numerical values in equation (37) gives:

$$V_{\mathrm{M}} \simeq 150 \text{ feet/second}$$

which represents on model scale in the wind tunnel, the design diving speed for the aircraft.

Thus, in terms of the aircraft, the outboard pair of ailerons alone give a reversal speed within the flight envelope of the aircraft, whilst both pairs of ailerons together give a marked fall in rolling power at the upper end of the speed range.

THIS DOCUMENT PROVIDED BY THE ABBOTT AEROSPACE
TECHNICAL LIBRARY
ABBOTTAEROSPACE.COM

TABLE 1

Matrix of Twist due to Applied Moment (Radians per lb. ft)

Applied moment section		1	2	3	4	5	6	7	8	9	10	11	12	13	y	η	$d\eta$
Measurement section	1	0·0100	0·0100	0·0100	0·0100	0·0100	0·0100	0·0100	0·0100	0·0100	0·0100	0·0100	0·0100	0·0100	0·1769	0·1206	0·0686
	2	0·0100	0·0180	0·0138	0·0123	0·0138	0·0128	0·0129	0·0141	0·0138	0·0163	0·0138	0·0147	0·0138	0·2775	0·1892	0·0686
	3	0·0100	0·0135	0·0250	0·0250	0·0250	0·0250	0·0250	0·0250	0·0250	0·0250	0·0250	0·0250	0·0250	0·3781	0·2578	0·0686
	4	0·0100	0·0123	0·0250	0·0357	0·0353	0·0359	0·0317	0·0367	0·0353	0·0350	0·0353	0·0372	0·0353	0·4786	0·3263	0·0686
	5	0·0100	0·0135	0·0250	0·0359	0·0520	0·0520	0·0520	0·0520	0·0520	0·0520	0·0520	0·0520	0·0520	0·5792	0·3449	0·0686
	6	0·0100	0·0127	0·0250	0·0357	0·0520	0·0757	0·0674	0·0678	0·0721	0·0771	0·0721	0·0761	0·0721	0·6797	0·4634	0·0686
Nacelle	7	0·0100	0·0132	0·0250	0·0315	0·0520	0·0662	0·0922	0·0821	0·0889	0·0948	0·0889	0·0900	0·0889	0·7967	0·5432	0·0909
Inboard aileron	8	0·0100	0·0145	0·0250	0·0365	0·0520	0·0694	0·0829	0·1259	0·1183	0·1224	0·1183	0·1143	0·1183	0·9136	0·6229	0·0686
	9	0·0100	0·0135	0·0250	0·0359	0·0520	0·0726	0·0895	0·1183	0·1630	0·1630	0·1630	0·1630	0·1630	1·0142	0·6915	0·0686
	10	0·0100	0·0134	0·0250	0·0375	0·0520	0·0786	0·0964	0·1224	0·1630	0·2223	0·2047	0·2047	0·2047	1·1147	0·7600	0·0686
Outboard aileron	11	0·0100	0·0135	0·0250	0·0359	0·0520	0·0726	0·0895	0·1183	0·1630	0·2047	0·3400	0·3400	0·3400	1·2153	0·8286	0·0686
	12	0·0100	0·0149	0·0250	0·0383	0·0520	0·0764	0·0892	0·1143	0·1630	0·2047	0·3400	0·5144	0·5144	1·3158	0·8972	0·0686
	13	0·0100	0·0135	0·0250	0·0359	0·0520	0·0726	0·0895	0·1183	0·1630	0·2047	0·3400	0·5144	0·7820	1·4164	0·9657	0·0686

Nose-up moment and nose-up twist positive

y = distance from roll axis to centre of section (feet)

$\eta = y \div$ (distance from roll axis to tip)

$d\eta$ = (width of section) $\div$ (distance from roll axis to tip)

THIS DOCUMENT PROVIDED BY THE ABBOTT AEROSPACE
TECHNICAL LIBRARY
ABBOTTAEROSPACE.COM

TABLE 2

Matrix of Twist due to Applied Load on the Q_0 *Line* (Radians per lb)

Applied load section	1	2	3	4	5	6	7	8	9	10	11	12	13
Measurement section 1	0	−0·0008	−0·0018	−0·0026	−0·0035	−0·0045	−0·0057	−0·0064	−0·0071	−0·0068	−0·0058	−0·0048	−0·0036
2		0	−0·0017	−0·0032	−0·0049	−0·0065	−0·0089	−0·0100	−0·0113	−0·0108	−0·0090	−0·0072	−0·0051
3			0	−0·0022	−0·0044	−0·0067	−0·0100	−0·0115	−0·0134	−0·0126	−0·0102	−0·0076	−0·0047
4				0	−0·0032	−0·0065	−0·0111	−0·0133	−0·0160	−0·0149	−0·0114	−0·0078	−0·0036
5					0	−0·0048	−0·0115	−0·0147	−0·0186	−0·0170	−0·0120	−0·0066	−0·0005
6						0	−0·0098	−0·0145	−0·0201	−0·0178	−0·0105	−0·0027	+0·0062
Nacelle 7							0	−0·0057	−0·0124	−0·0097	−0·0008	+0·0087	+0·0196
Inboard aileron 8								0	−0·0092	−0·0055	+0·0067	+0·0196	+0·0345
9									0	+0·0049	+0·0206	+0·0373	+0·0566
10										0	+0·0215	+0·0442	+0·0706
Outboard aileron 11											0	+0·0348	+0·0750
12												0	+0·0609
13	0	0	0	0	0	0	0	0	0	0	0	0	0

Download and nose-up positive

THIS DOCUMENT PROVIDED BY THE ABBOTT AEROSPACE
TECHNICAL LIBRARY
ABBOTTAEROSPACE.COM

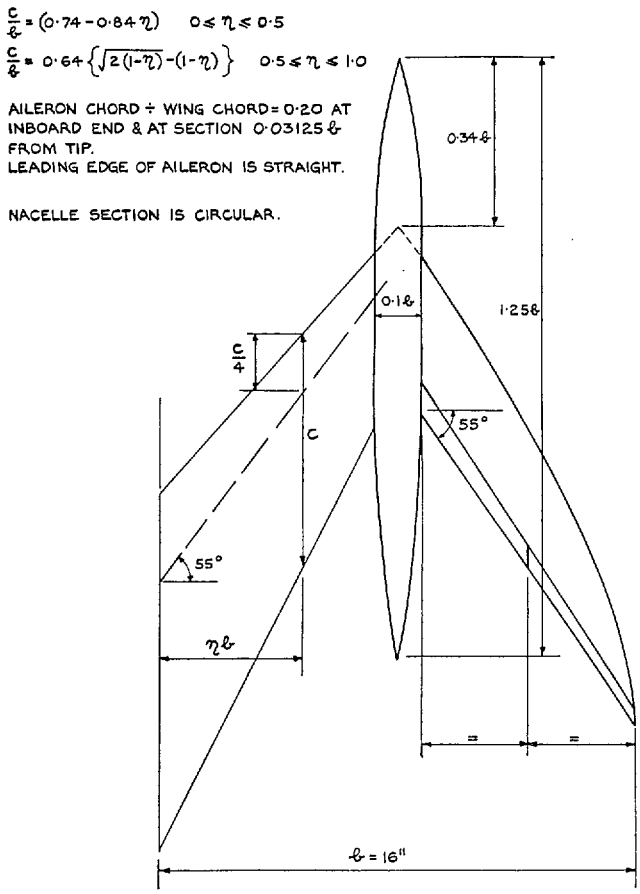

FIG. 1. Wing geometry.

THIS DOCUMENT PROVIDED BY THE ABBOTT AEROSPACE
TECHNICAL LIBRARY
ABBOTTAEROSPACE.COM

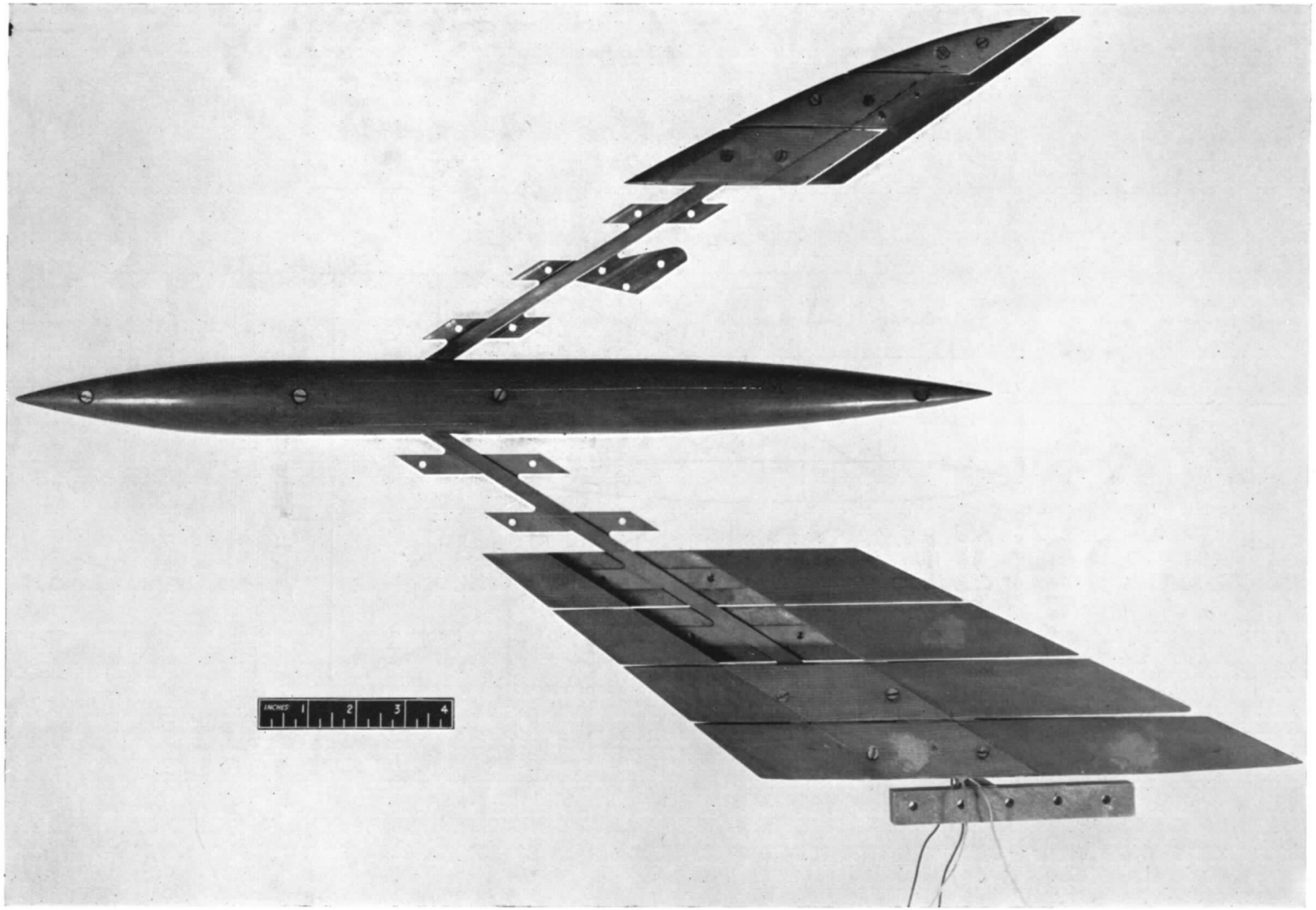

FIG. 2. Wing construction.

THIS DOCUMENT PROVIDED BY THE ABBOTT AEROSPACE
TECHNICAL LIBRARY
ABBOTTAEROSPACE.COM

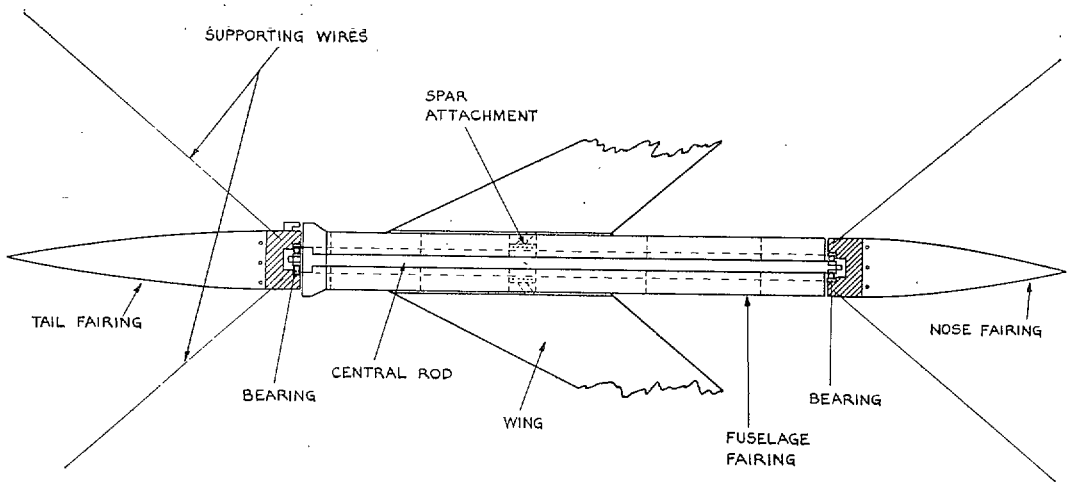

FIG. 3. Rig for wind-tunnel tests.

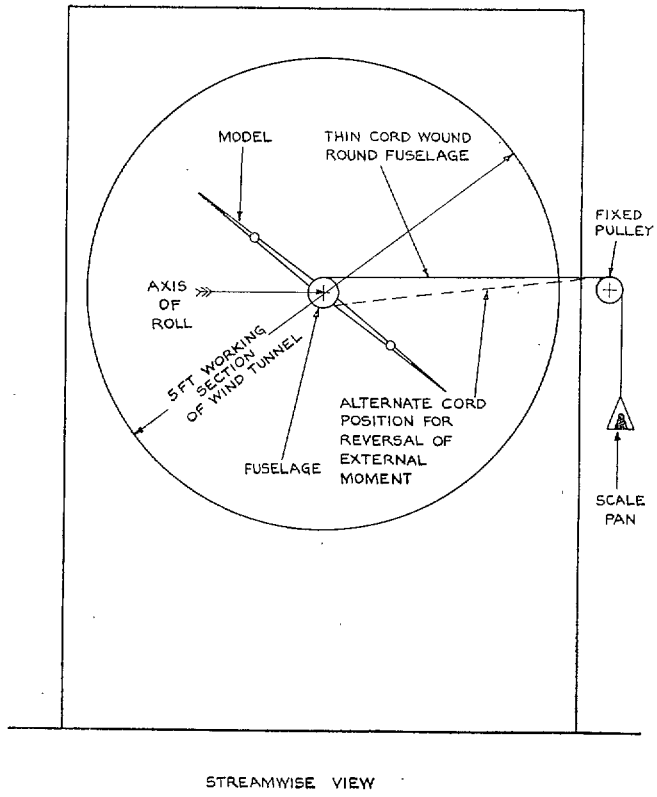

FIG. 4. Rig for external rolling moments.

THIS DOCUMENT PROVIDED BY THE ABBOTT AEROSPACE
TECHNICAL LIBRARY
ABBOTTAEROSPACE.COM

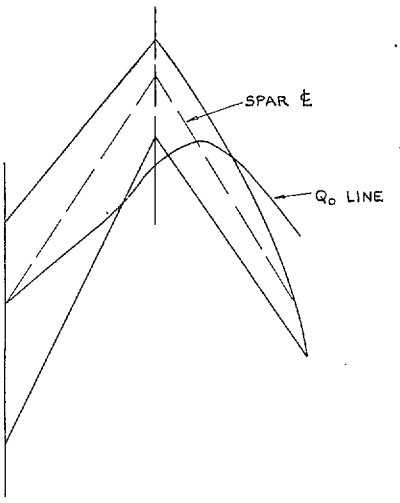

FIG. 5. Position of Q_0 line.

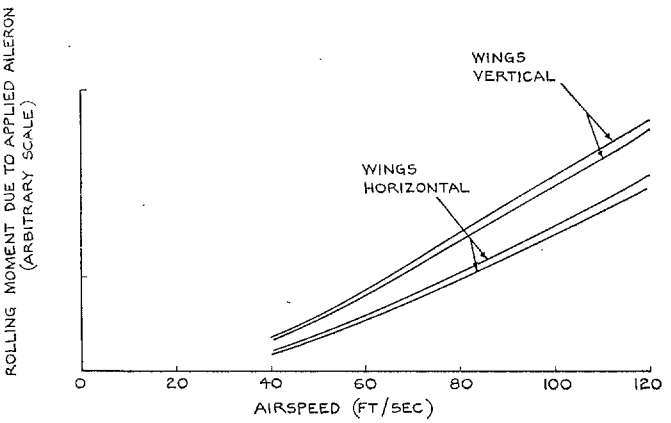

FIG. 6. Gravitational effect on rolling moment.

THIS DOCUMENT PROVIDED BY THE ABBOTT AEROSPACE
TECHNICAL LIBRARY
ABBOTTAEROSPACE.COM

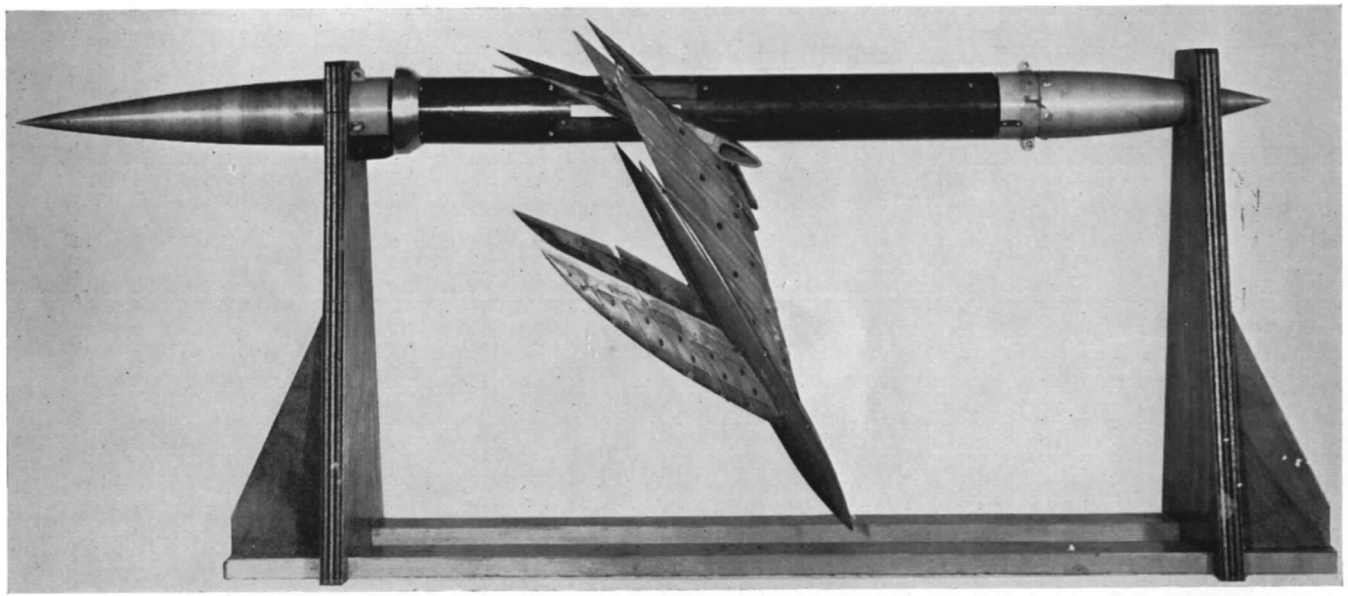

FIG. 7. Model after divergence.

THIS DOCUMENT PROVIDED BY THE ABBOTT AEROSPACE
TECHNICAL LIBRARY
ABBOTTAEROSPACE.COM

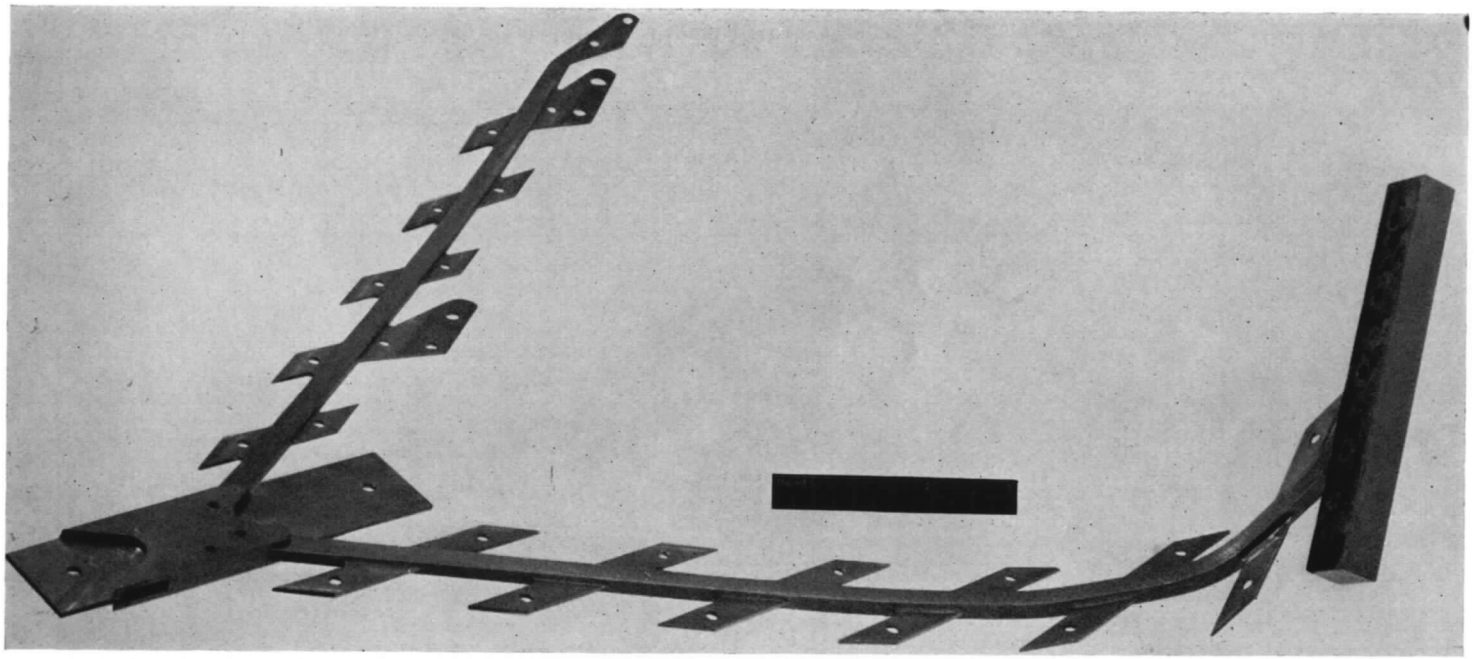

FIG. 8. Model spar after divergence.

THIS DOCUMENT PROVIDED BY THE ABBOTT AEROSPACE
TECHNICAL LIBRARY
ABBOTTAEROSPACE.COM

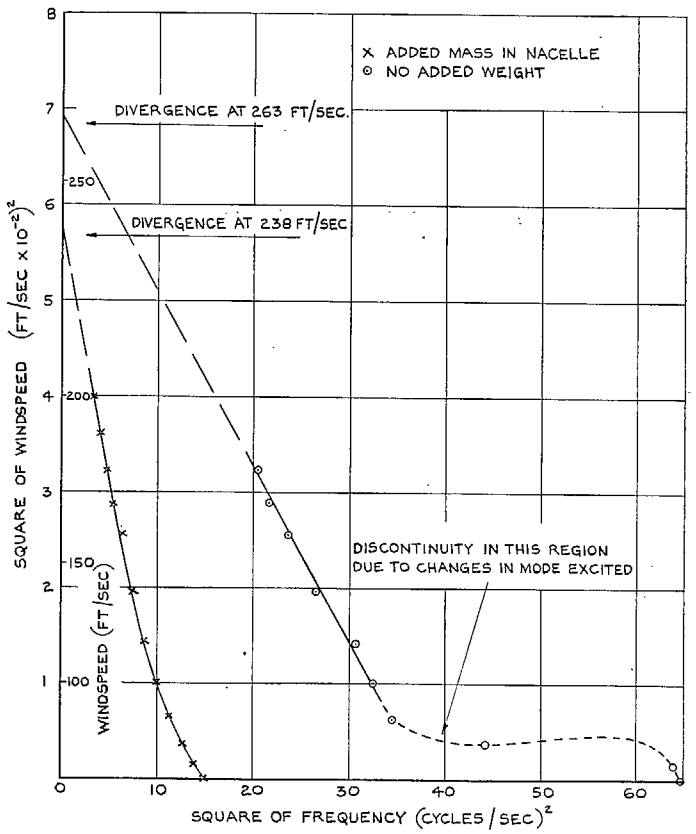

FIG. 9. Divergence test results.

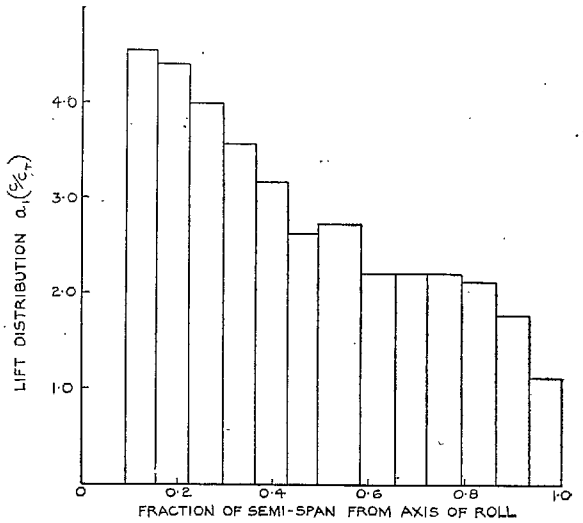

FIG. 10a. Wing lift distribution.

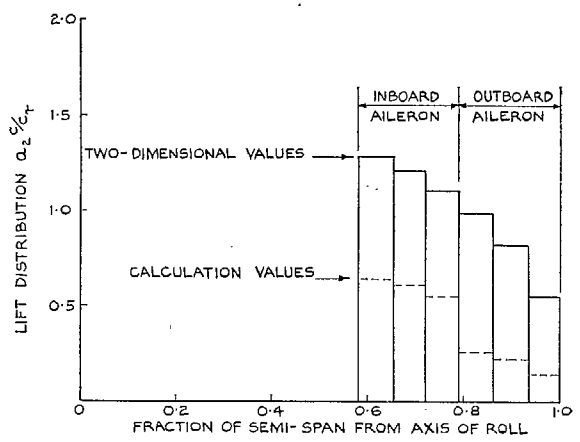

FIG. 10b. Aileron lift distribution.

THIS DOCUMENT PROVIDED BY THE ABBOTT AEROSPACE
TECHNICAL LIBRARY
ABBOTTAEROSPACE.COM

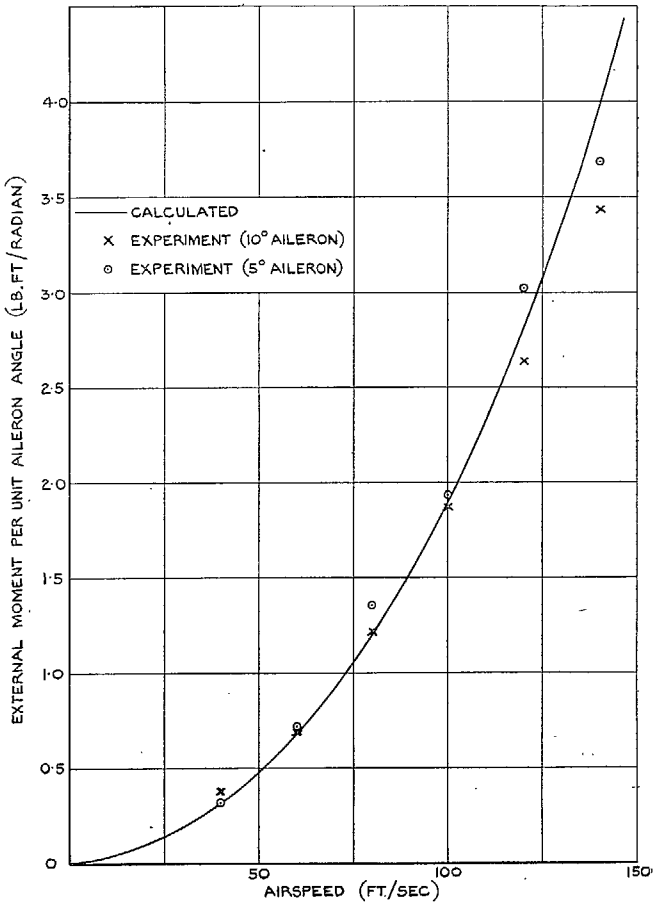

FIG. 11. Variation of external moment per unit aileron angle with airspeed (inboard ailerons).

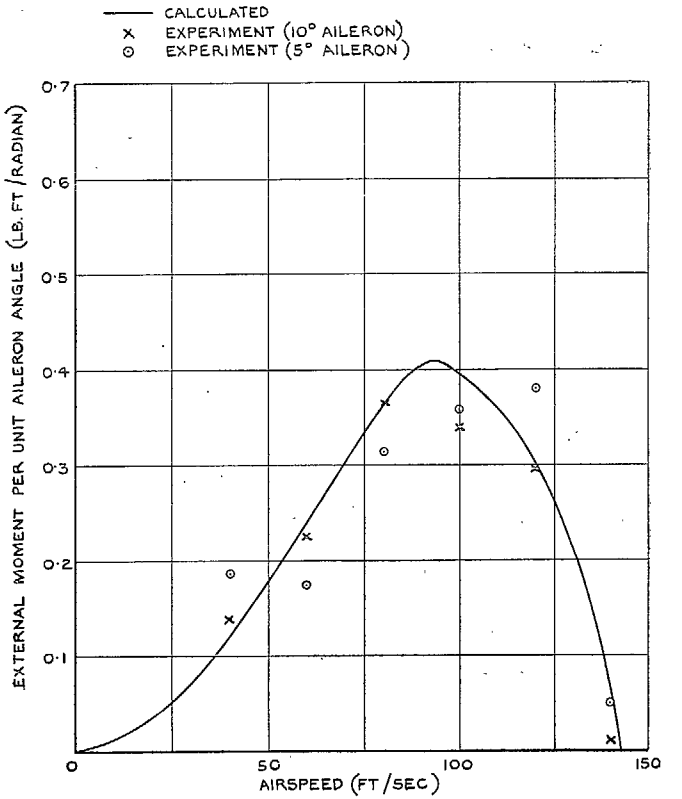

FIG. 12. Variation of external moment per unit aileron angle with airspeed (outboard ailerons).

THIS DOCUMENT PROVIDED BY THE ABBOTT AEROSPACE
TECHNICAL LIBRARY
ABBOTTAEROSPACE.COM

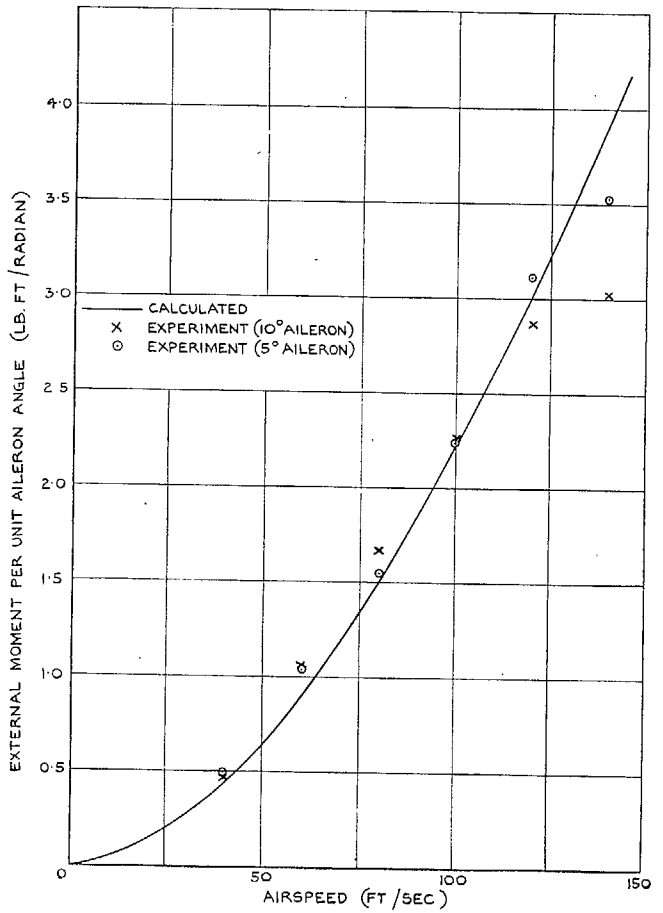

FIG. 13. Variation of external moment per unit aileron angle with airspeed (both pairs of ailerons).

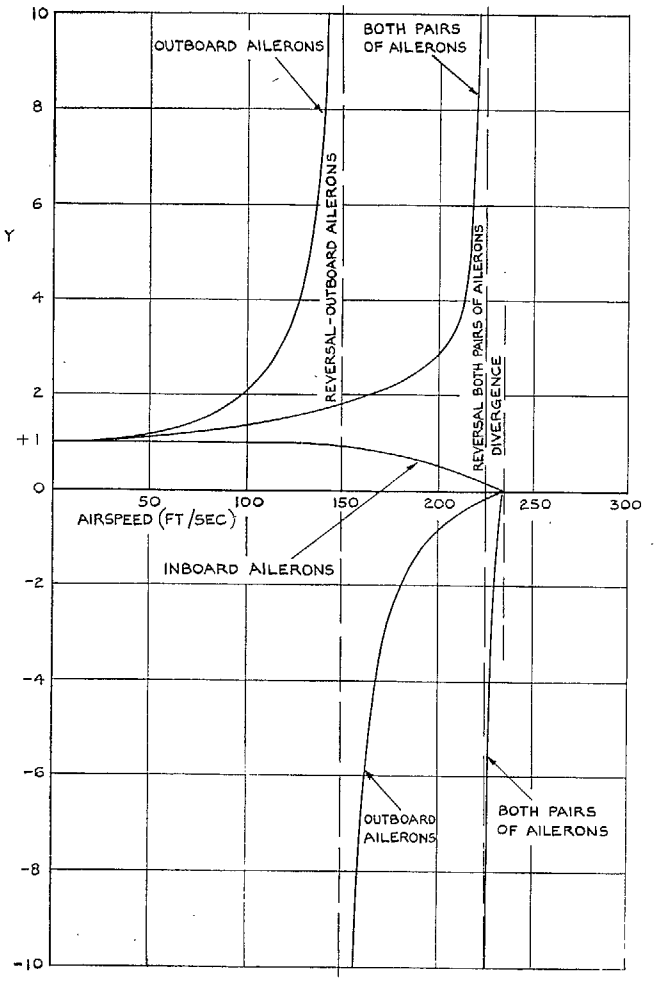

FIG. 14. Variation of Y with airspeed.

THIS DOCUMENT PROVIDED BY THE ABBOTT AEROSPACE
TECHNICAL LIBRARY
ABBOTTAEROSPACE.COM

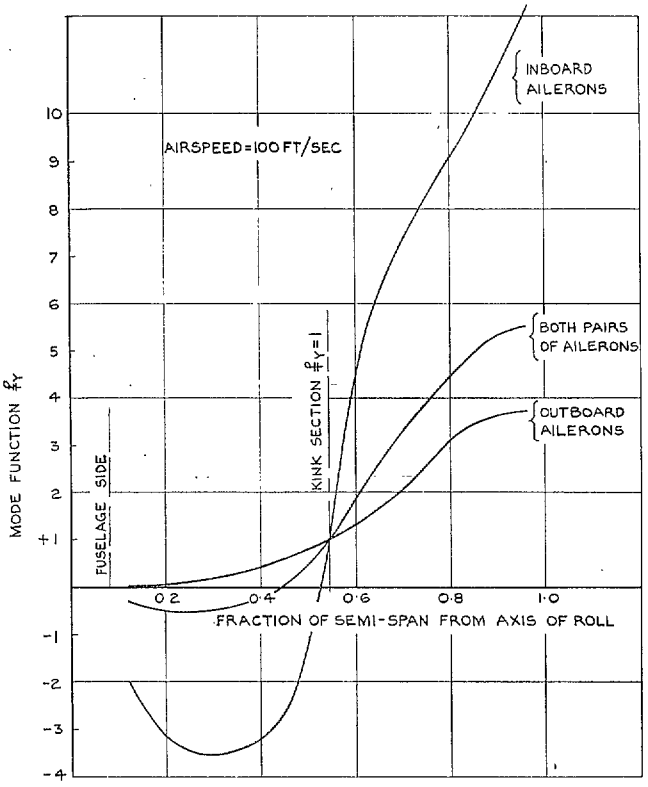

FIG. 15. Mode shape due to applied aileron (no roll).

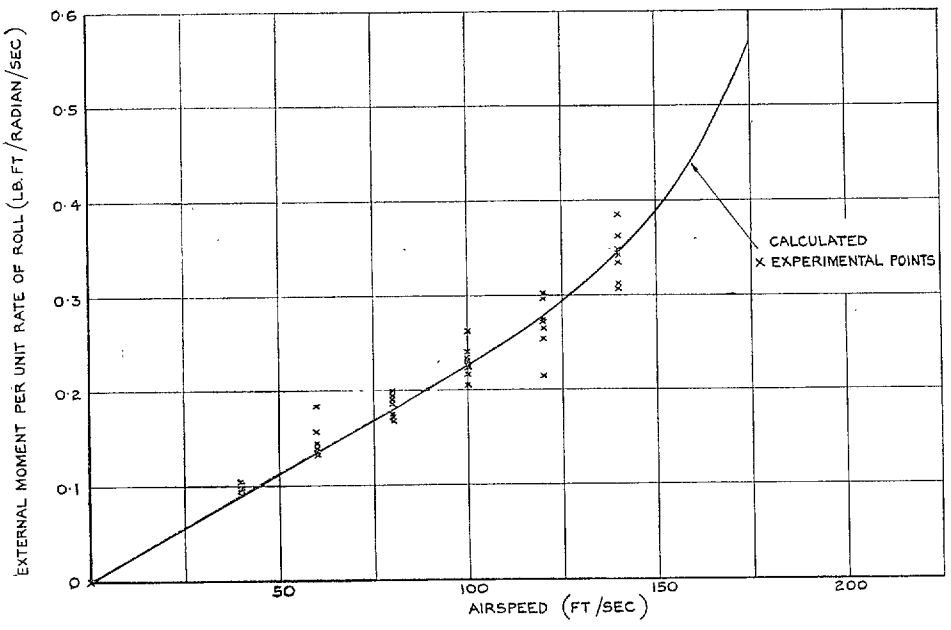

FIG. 16. Variation of external rolling moment per unit rate of roll with airspeed.

THIS DOCUMENT PROVIDED BY THE ABBOTT AEROSPACE
TECHNICAL LIBRARY
ABBOTTAEROSPACE.COM

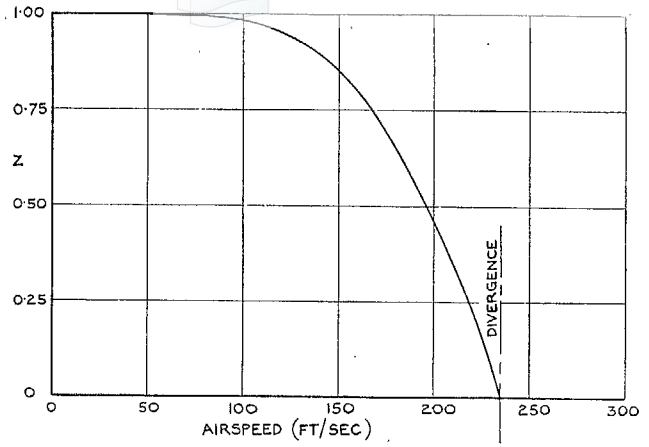

FIG. 17. Variation of Z with airspeed.

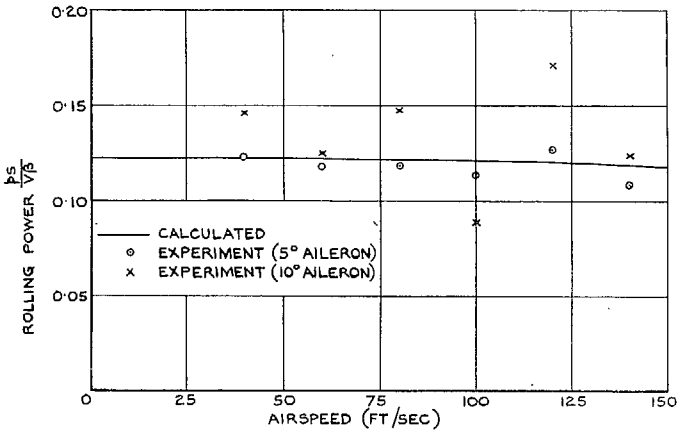

FIG. 19. Rolling power—inboard ailerons.

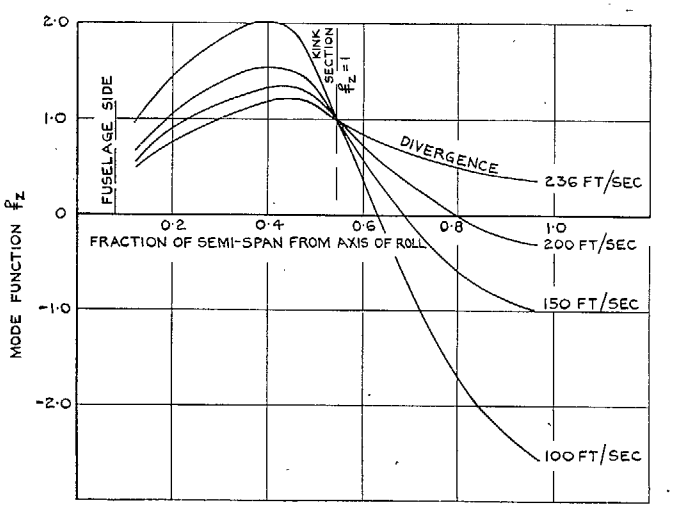

FIG. 18. Mode shape due to rate of roll (no aileron).

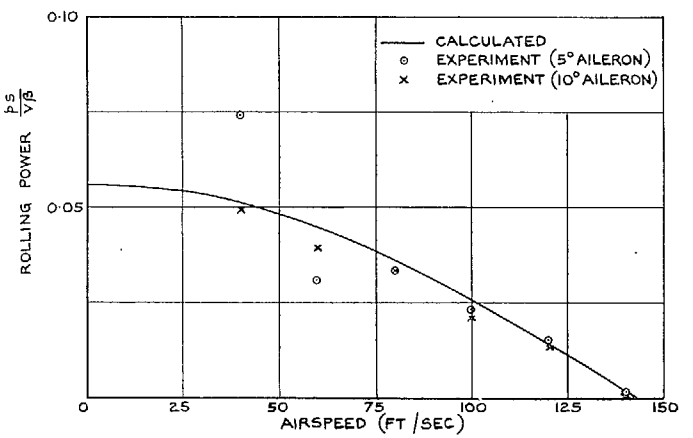

FIG. 20. Rolling power—outboard ailerons.

THIS DOCUMENT PROVIDED BY THE ABBOTT AEROSPACE
TECHNICAL LIBRARY
ABBOTTAEROSPACE.COM

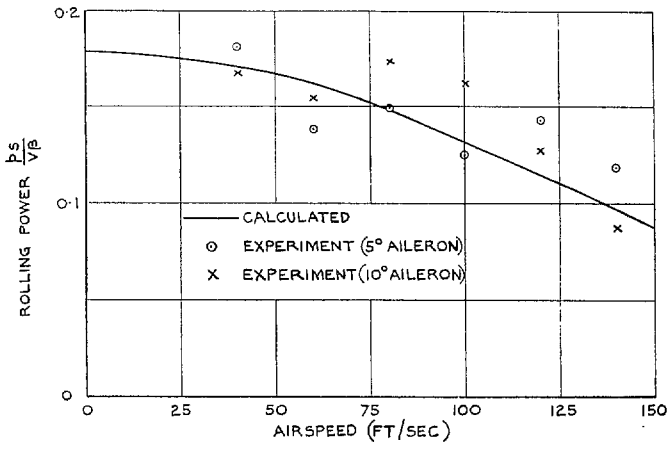

FIG. 21. Rolling power—both pairs of ailerons.

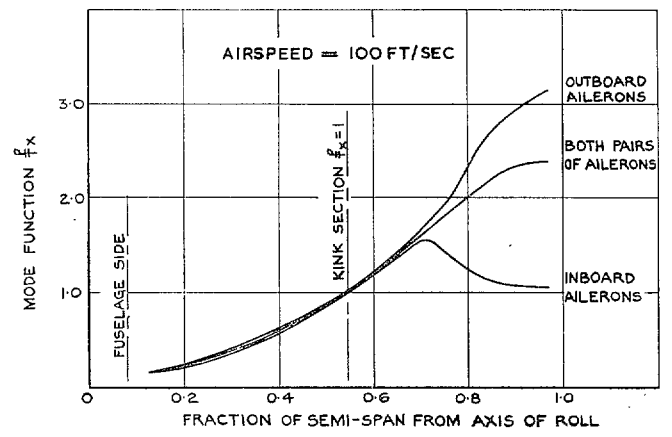

FIG. 22. Mode shape in free roll.

(89023) Wt. 65/1418 K5 5/64 Hw.

THIS DOCUMENT PROVIDED BY THE ABBOTT AEROSPACE
TECHNICAL LIBRARY
ABBOTTAEROSPACE.COM

Publications of the Aeronautical Research Council

ANNUAL TECHNICAL REPORTS OF THE AERONAUTICAL RESEARCH COUNCIL (BOUND VOLUMES)

1942 Vol. I. Aero and Hydrodynamics, Aerofoils, Airscrews, Engines. 75*s.* (post 2*s.* 9*d.*)
Vol. II. Noise, Parachutes, Stability and Control, Structures, Vibration, Wind Tunnels. 47*s.* 6*d.* (post 2*s.* 3*d.*)

1943 Vol. I. Aerodynamics, Aerofoils, Airscrews. 80*s.* (post 2*s.* 6*d.*)
Vol. II. Engines, Flutter, Materials, Parachutes, Performance, Stability and Control, Structures. 90*s.* (post 2*s.* 9*d.*)

1944 Vol. I. Aero and Hydrodynamics, Aerofoils, Aircraft, Airscrews, Controls. 84*s.* (post 3*s.*)
Vol. II. Flutter and Vibration, Materials, Miscellaneous, Navigation, Parachutes, Performance, Plates and Panels, Stability, Structures, Test Equipment, Wind Tunnels. 84*s.* (post 3*s.*)

1945 Vol. I. Aero and Hydrodynamics, Aerofoils. 130*s.* (post 3*s.* 6*d.*)
Vol. II. Aircraft, Airscrews, Controls. 130*s.* (post 3*s.* 6*d.*)
Vol. III. Flutter and Vibration, Instruments, Miscellaneous, Parachutes, Plates and Panels, Propulsion. 130*s.* (post 3*s.* 3*d.*)
Vol. IV. Stability, Structures, Wind Tunnels, Wind Tunnel Technique. 130*s.* (post 3*s.* 3*d.*)

1946 Vol. I. Accidents, Aerodynamics, Aerofoils and Hydrofoils. 168*s.* (post 3*s.* 9*d.*)
Vol. II. Airscrews, Cabin Cooling, Chemical Hazards, Controls, Flames, Flutter, Helicopters, Instruments and Instrumentation, Interference, Jets, Miscellaneous, Parachutes. 168*s.* (post 3*s.* 3*d.*)
Vol. III. Performance, Propulsion, Seaplanes, Stability, Structures, Wind Tunnels. 168*s.* (post 3*s.* 6*d.*)

1947 Vol. I. Aerodynamics, Aerofoils, Aircraft. 168*s.* (post 3*s.* 9*d.*)
Vol. II. Airscrews and Rotors, Controls, Flutter, Materials, Miscellaneous, Parachutes, Propulsion, Seaplanes, Stability, Structures, Take-off and Landing. 168*s.* (post 3*s.* 9*d.*)

1948 Vol. I. Aerodynamics, Aerofoils, Aircraft, Airscrews, Controls, Flutter and Vibration, Helicopters, Instruments, Propulsion, Seaplane, Stability, Structures, Wind Tunnels. 130*s.* (post 3*s.* 3*d.*)
Vol. II. Aerodynamics, Aerofoils, Aircraft, Airscrews, Controls, Flutter and Vibration, Helicopters, Instruments, Propulsion, Seaplane, Stability, Structures, Wind Tunnels. 110*s.* (post 3*s.* 3*d.*)

Special Volumes

Vol. I. Aero and Hydrodynamics, Aerofoils, Controls, Flutter, Kites, Parachutes, Performance, Propulsion, Stability. 126*s.* (post 3*s.*)
Vol. II. Aero and Hydrodynamics, Aerofoils, Airscrews, Controls, Flutter, Materials, Miscellaneous, Parachutes, Propulsion, Stability, Structures. 147*s.* (post 3*s.*)
Vol. III. Aero and Hydrodynamics, Aerofoils, Airscrews, Controls, Flutter, Kites, Miscellaneous, Parachutes, Propulsion, Seaplanes, Stability, Structures, Test Equipment. 189*s.* (post 3*s.* 9*d.*)

Reviews of the Aeronautical Research Council

1939–48 3*s.* (post 6*d.*) 1949–54 5*s.* (post 5*d.*)

Index to all Reports and Memoranda published in the Annual Technical Reports

1909–1947 R. & M. 2600 (out of print)

Indexes to the Reports and Memoranda of the Aeronautical Research Council

Between Nos. 2351–2449	R. & M. No. 2450 2*s.* (post 3*d.*)
Between Nos. 2451–2549	R. & M. No. 2550 2*s.* 6*d.* (post 3*d.*)
Between Nos. 2551–2649	R. & M. No. 2650 2*s.* 6*d.* (post 3*d.*)
Between Nos. 2651–2749	R. & M. No. 2750 2*s.* 6*d.* (post 3*d.*)
Between Nos. 2751–2849	R. & M. No. 2850 2*s.* 6*d.* (post 3*d.*)
Between Nos. 2851–2949	R. & M. No. 2950 3*s.* (post 3*d.*)
Between Nos. 2951–3049	R. & M. No. 3050 3*s.* 6*d.* (post 3*d.*)
Between Nos. 3051–3149	R. & M. No. 3150 3*s.* 6*d.* (post 3*d.*)

HER MAJESTY'S STATIONERY OFFICE

from the addresses overleaf

THIS DOCUMENT PROVIDED BY THE ABBOTT AEROSPACE
TECHNICAL LIBRARY
ABBOTTAEROSPACE.COM

© *Crown copyright* 1964

Printed and published by
HER MAJESTY'S STATIONERY OFFICE

To be purchased from
York House, Kingsway, London W.C.2
423 Oxford Street, London W.1
13A Castle Street, Edinburgh 2
109 St. Mary Street, Cardiff
39 King Street, Manchester 2
50 Fairfax Street, Bristol 1
35 Smallbrook, Ringway, Birmingham 5
80 Chichester Street, Belfast 1
or through any bookseller

Printed in England

S.O. Code No. 23-3362